JOURNAL OF CATALYSIS 89, 185–195 (1984)

Characterization of 12-Tungstophosphoric Acid and Related Salts Using Photoacoustic Spectroscopy in the Infrared Region

II. Interactions with Pyridine

J. G. HIGHFIELD AND J. B. MOFFAT[1]

Department of Chemistry, University of Waterloo, Waterloo, Ontario, Canada N2L 3G1

Received January 4, 1984; revised May 8, 1984

Photoacoustic spectroscopy in the infrared region (PAS–FTIR) has been used to study the interactions of pyridine with 12-tungstophosphoric acid, $H_3PW_{12}O_{40}$, and the respective NH_4^+, Al^{3+}, Na^+, and pyridinium salts, heteropoly compounds which show interesting trends in activity and selectivity in the conversion of methanol to hydrocarbons. At room temperature, the parent acid readily sorbs up to 6 pyridine(py) molecules per Keggin unit, i.e., $PW_{12}O_{40}^{3-}$, to form the dimer ion salt $(py_2H)_3PW_{12}O_{40}$, and exchange studies have revealed that the pyridine molecules in the dimer ion are equivalent. Above 100°C, pyridine is desorbed to yield the pyridinium salt, $(pyH)_3PW_{12}O_{40}$. Sorption of pyridine into the salts is not as facile as NH_3, showing marked dependence on the cation and temperature. Steric factors are evidently important in controlling the diffusion rate of this larger probe molecule into their bulk structures. The existence of the salts in partial (Brønsted) acid form has been confirmed, and the results of pyridine desorption studies indicate qualitative differences in their acid strengths.

INTRODUCTION

Recent work (*1*) has shown that when a photoacoustic (PAS) cell is interfaced to a conventional Fourier Transform Infrared (FTIR) spectrometer, good quality optical absorption spectra can be readily obtained from catalyst samples in opaque, fine powder form. PAS–FTIR effectively circumvents the practical and interpretative difficulties associated with the pressed disk technique in conventional transmission spectroscopy. The technique was found to provide valuable qualitative and quantitative information concerning the structure, thermal stability, and acidity of 12-tungstophosphoric acid and related salts; heteropoly compounds which show interesting trends in activity and selectivity in methanol conversion (*2, 3*). When the catalysts are exposed to gaseous ammonia, this small basic molecule readily penetrates into their bulk structure and, thus, serves as a good (quantitative) probe of total acidity. However, it is generally considered that ammonia is too strong a base to be of great value in selective poisoning studies (*4*), although it may be used as a stepwise poison by dosing small quantities successively and monitoring its mode of interaction with the catalyst by spectroscopic techniques, e.g., as in the case of the aluminum salt reported earlier (*1*). Nevertheless, the use of a weaker base such as pyridine is generally preferred (*4*). Moreover, from molecular size considerations, methanol may be expected to show (bulk) diffusional behavior intermediate between that of ammonia and pyridine. Hence, studies of the interaction of these heteropoly compounds with the latter base may yield useful complementary information concerning both their acidity (acid type and strength) and bulk structure, e.g., the interstitial (cation) space.

Previous work using conventional ir transmission spectroscopy has indicated

[1] To whom correspondence should be addressed.

0021-9517/84 $3.00

that 12-tungstophosphoric acid sorbs large quantities of pyridine (py) at room temperature, possibly resulting in the formation of the pyridinium–pyridine (pyH^+–py) dimer ion (*5*).

In this paper, we report the application of PAS–FTIR to study the interactions of gaseous pyridine with 12-tungstophosphoric acid, $H_3PW_{12}O_{40}$, and the respective ammonium, aluminum, sodium, and pyridinium salts of the parent acid.

EXPERIMENTAL

PAS–FTIR spectra from 4000 to 550 cm^{-1} were recorded on a Bomem DA3.02 Fourier Transform infrared spectrometer equipped with a photoacoustic detector. The instrumental layout and operating conditions have previously been described (*1*), as have the preparation and physicochemical characterization of the heteropoly compounds under investigation (*2, 3*). The pyridinium salt was prepared by adding pyridine to an aqueous solution of $H_3PW_{12}O_{40}$ in stoichiometric proportions.

Sample pretreatment was performed on a conventional vacuum system capable of an ultimate dynamic vacuum of 10^{-5} Torr. Reagents pyridine (J. T. Baker Chemical Co.) ammonia (anhydrous, 99.99%; Matheson), pyridine-d_5 and D_2O (99.5% and 99.7% minimum isotopic purity, respectively; Merck, Sharpe & Dohme) were subjected to several freeze–pump–thaw cycles to remove contaminant gases prior to use. Pyridines were kept dry over activated molecular sieve 3A, while ammonia was also predried by trap-to-trap distillation. Uptakes were measured volumetrically (to a precision of typically ±0.5%) and expressed, for convenience, as molecules sorbed per Keggin unit ($PW_{12}O_{40}^{3-}$ ion) calculated on a dry weight basis. Powder X-ray diffraction data were obtained using a Philips diffractometer (Model PW-1011/60) at 40 kV and 30 mA using Ni-filtered Cu$K\alpha$ radiation. Elemental analyses (samples preevacuated at 150°C) were obtained from Galbraith Laboratories Inc.

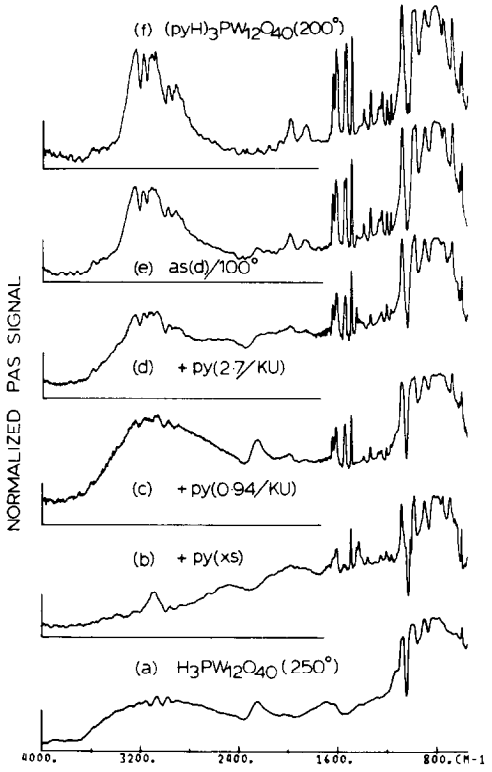

FIG. 1. (a) $H_3PW_{12}O_{40}$ (preevacuated at 250°C); (b) after exposure to excess pyridine at 25°C and evacuation; (c) as (a) exposed to a controlled dose of pyridine (0.94 py/KU); (d) as (a) exposed to a larger dose of pyridine (2.7 py/KU); (e) as (d) after heating under static vacuum at 100°C; (f) pyridinium salt, $(pyH)_3PW_{12}O_{40}$ (preevacuated at 200°C) for comparison.

RESULTS

1. Pyridine on $H_3PW_{12}O_{40}$

After preevacuation at 250°C (Fig. 1a), exposure of $H_3PW_{12}O_{40}$ to excess pyridine at 25°C resulted in a fairly rapid initial uptake, followed by a slow continuous sorption reaching a total limiting value of ~6 py/KU in 1 h. The PAS spectrum after evacuation at 25°C (Fig. 1b) exhibits new bands associated with sorbed pyridine (1700–1100 cm^{-1}) and the band envelope characteristic of the Keggin unit (*1*) in the range 1100–600 cm^{-1}, superimposed on a background whose intensity continuously increases with decrease in wavenumber.

On preliminary inspection, the spectrum indicates that the formation of the pyridinium ion is inhibited. The background continuum (also present in $H_3PW_{12}O_{40}$) has already been attributed to the presence of mobile protons (*1*), and a band at 1540 cm^{-1} characteristic of the pyridinium ion is hardly detectable. Instead, major bands are observed at 1605, 1489, 1443, and 1425 cm^{-1}, indicative of the association of pyridine in hydrogen-bonded form(s) (*6*). However, when dosed in controlled amount (0.94 py/KU) at 25°C (completely sorbed in 15 min), the PAS spectrum (Fig. 1c) exhibits strong bands at 1640, 1610, 1537, and 1485 cm^{-1}, characteristic of protonated pyridine. Comparison of relative peak intensities with those of pyridinium salts in the literature (*7*) and the absence of bands characteristic of other types of bound pyridine (*6*) indicates that all the sorbed pyridine has been converted to pyridinium ion. Upon dosing the stoichiometric amount (3 py/KU) at 25°C, most of the pyridine (2.7 py/KU) was sorbed in ~2.5 h. The PAS spectrum (Fig. 1d) reveals the presence of the pyridinium ion as the major species but the 1540-cm^{-1} band appears selectively suppressed and a band characteristic of H-bonded pyridine is also present at 1443 cm^{-1}. When this sample was heated under static vacuum up to 100°C, the PAS spectrum (Fig. 1e) showed a significant enhancement of bands attributable to the pyridinium ion, and attenuation of both the 1443-cm^{-1} band and the background continuum, a result which implies the conversion of that fraction of pyridine in H-bonded form to the protonated species. The spectrum now resembles closely that of the pyridinium salt (Fig. 1f). Upon exposure of the same sample to excess pyridine at 25°C (sorbing a further 2.6py/KU in 0.5 h, an amount equivalent to that already sorbed) the PAS spectrum appears almost identical to that obtained by direct exposure to excess pyridine at 25°C without the intermediate heating step (Fig. 1b). On evacuation at 100°C, the spectrum characteristic of the pyridinium salt is regenerated. This series of experiments demonstrates that when dosed in substoichiometric amounts, pyridine readily penetrates into the bulk of $H_3PW_{12}O_{40}$ at 25°C to form the (partial) pyridinium salt. At stoichiometric loading or above, however, pyridine interacts with the pyridinium ion to form a H-bonded complex, possibly involving two pyridine molecules and one proton. A similar conclusion has been reached by other workers based on less extensive studies by conventional FTIR transmission spectroscopy (*5*). The occurrence of the $(py_2H)^+$ ion in solution has been established spectroscopically by Clements and Wood (*8*), and certain features in their ir transmission spectrum appear to correlate with those in the PAS spectrum of the system examined here. Two broad absorption bands centered at 2500 and 2100 cm^{-1} in the former may correspond to similar bands in the PAS spectrum, centered at 2500 and 2000 cm^{-1} (Fig. 1b). The above authors attribute these features to N–H stretching vibrations without any explanation as to the occurrence of the doublet. In addition, they observe selective suppression of the band at 1540 cm^{-1}, consistent with our observations. Parry (*6*) states that this band is diagnostic of the N–H grouping and is, hence, unique to the pyridinium ion. More specifically, Cook (*7*) has assigned it to an in-plane skeletal deformation mode (ν_{19b}) which includes the N–H grouping. Hence, the suppression of this band, together with the simultaneous reduction of the N–H stretching band at 3100 cm^{-1} may be expected to result from the formation of a species such as $(pyH\ldots py)^+$. In support of this, the background continuum, which develops in the presence of excess pyridine, is not now considered to originate from intermolecular migration of protons as in the case of $H_3PW_{12}O_{40}$ (*1*) but is more likely related to the pyridinium/pyridine complex. From extensive studies in solution, Zundel (*9*) has concluded that ir continua can result from the induced-dipole interactions of easily po-

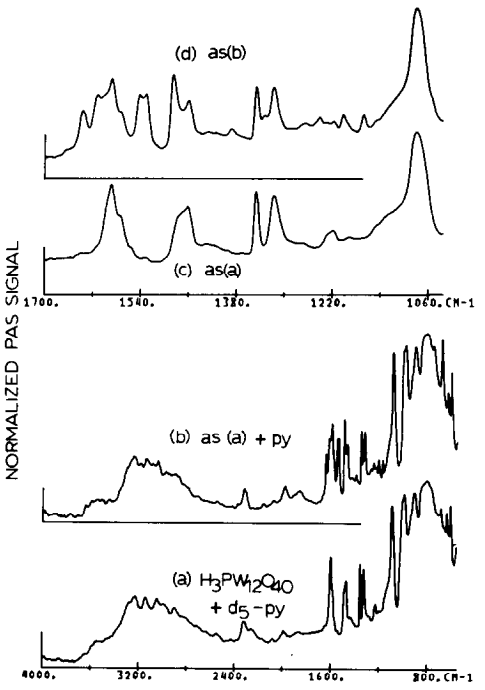

FIG. 2. (a) $H_3PW_{12}O_{40}$ (preevacuated at 250°C) after sorption of d_5-pyridine (2.5 d_5-py/KU) at 150°C; (b) as (a) after sorption of pyridine (2.5 py/KU) at 25°C and subsequent evacuation at 180°C; (c) detail of (a) with wavenumber scale expanded for clarity; (d) corresponding detail of (b).

larizable H-bonds [in groupings such as $(BH \ldots B)^+$, where B = base] with their environment. In the case of pyridine, the proton affinity is probably large enough to create a double-minimum potential well. Two limiting configurations may be hypothesized for the $(py_2H)^+$ species, one in which the proton is shared by and can oscillate between two equivalent pyridine molecules $(py \ldots H \ldots py)^+$, and a second in which the proton may be associated with the original pyridine molecule, with strong interaction of the second pyridine molecule being precluded, possibly by steric effects. In order to distinguish between these two forms, a simple pyridine exchange study was carried out. A sample of $H_3PW_{12}O_{40}$ was exposed to an excess of d_5-pyridine at 150°C until a significant uptake was measured (2.5 py/KU) and the remainder was removed by pumping. The PAS spectrum (Fig. 2a) shows features characteristic of the d_5-pyH^+ pyridinium ion, particularly in the region 1600–1200 cm^{-1} (Fig. 2c), which contains bands originating from ring-deformation modes (*7*). The peaks centered at 1586, 1468, 1346, and 1316 cm^{-1} are considered to be the deuterated analogs of those at 1620 (ν_{8a}, ν_{8b}), 1537 (ν_{19b}), 1485 (ν_{19a}), and 1333 (ν_3) cm^{-1}, respectively, the former positions and assignments correlating well with those reported by Clements and Wood (*8*). After an almost equivalent amount of pyridine (2.5 py/KU) was sorbed onto this sample at 25°C and the temperature raised slowly to 180°C under static vacuum, a similar amount was desorbed. After evacuation, the PAS spectrum (Fig. 2b) showed clear evidence for pyridine exchange. In the region 1700–1200 cm^{-1} (Fig. 2d), the original peaks are attenuated and new peaks characteristic of the undeuterated (H_5–pyH^+) pyridinium ion appear, including the doublet centered at 1537 cm^{-1}. The peak area ratio A_{1537}/A_{1080} indicates that almost half the original d_5-pyridine has been exchanged (see later), providing strong evidence in favor of the formation of a dimer ion in which the two pyridine molecules are equivalent. Successive treatment with pyridine as above resulted in its continuous enrichment at the expense of the d_5-analog.

Concerning the possibilities of using pyridine as a quantitative probe of Brønsted acidity in the heteropoly salts, in complementary manner to NH_3 (*1*), it appears necessary that the calibration curve be constructed by dosing pyridine onto $H_3PW_{12}O_{40}$ and heating to a temperature at which the dimer is unstable, i.e., above 100°C. Certainly, there is no spectral evidence for coordinately bound pyridine (one would expect residual bands at 1580 and 1450 cm^{-1}) characteristic of Lewis acidity (*6*), a result consistent with that obtained using NH_3 (*1*). Evidence both in the literature (*6, 7*) and in previous PAS spectra indicates that the 1537-cm^{-1} band is unique to the pyridinium ion and is, hence, the most

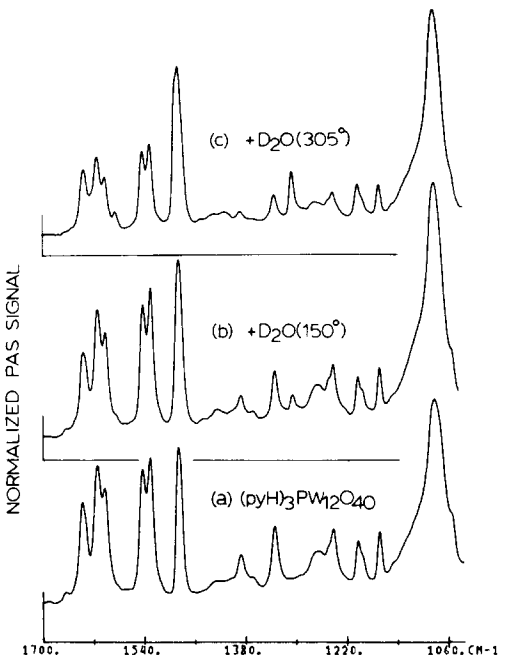

FIG. 3. (a) pyridinium salt, spectral detail illustrating splitting of bands centered at 1610 and 1537 cm^{-1}; (b) as (a) after exposure to D_2O at 150°C; (c) as (b) after exposure to D_2O at 305°C.

suitable analyte peak for quantitative analysis. The P–O stretching fundamental at 1080 cm^{-1} was once again selected as reference (*1*). After dosing pyridine successively at 25°C onto $H_3PW_{12}O_{40}$ (preevacuated at 250°C) and heating above 100°C in a closed system (to convert any dimer to monomer), the calibration curve for the peak area ratio A_{1537}/A_{1080} versus sorbed pyridine showed good linearity up to 1.5py/KU, with negative deviation at higher loadings characteristic of the onset of signal saturation.

Compared to that of the $NH_3/H_3PW_{12}O_{40}$ system (*1*), this curve shows an earlier onset, and greater degree, of signal saturation despite the optical extinction coefficients (at the peak maxima) of the respective analyte peaks being similar, as indicated by their peak heights with respect to that of the reference peak at equivalent (and low) analyte loadings. This apparent inconsistency is believed to be associated with differences in bandshape, as semiquantitative theoretical calculation indicates that saturation effects would be expected to be manifest under the experimental conditions utilized here. This phenomenon, which is considered a minor analytical problem, is discussed in some detail elsewhere (*10*).

Particularly intriguing features in the PAS spectra of the pyridinium salt (Fig. 3a) are the splitting of the peaks centered at 1610 and 1537 cm^{-1} into doublets at 1615, 1604 cm^{-1}, and 1543, 1531 cm^{-1}, respectively, details not reported elsewhere in the literature. If the assignments of Cook (*7*) are correct, these bands are in-plane skeletal deformation modes ν_{8b} (B_1) and ν_{19b} (B_1), respectively, and, hence, nondegenerate. N-deuteration, effected by exposure of this salt to D_2O (Figs. 3b,c), causes significant reduction in intensity of these doublets and the development of new bands at 1585 and 1490 cm^{-1}, confirming that both doublets are associated with the N–H grouping. Changes observed in these bands as pyridine is dosed stepwise onto $H_3PW_{12}O_{40}$ suggest that the splittings are associated with distortion of the crystal structure. Initially, only single bands are evident at 1610 and 1537 cm^{-1} but splitting becomes just discernible at ~1 py/KU (Figs. 4a,b). On further addition, the doublets develop progressively until the spectrum ultimately resembles closely that of the pyridinium salt (Figs. 4c,d,e). In support of this, the XRD pattern of the salt is not characteristic of a cubic system but shows many peaks, implying a lowering of crystal symmetry (*11*), possibly in order to facilitate the accommodation of these relatively large cations. However if, as the results suggest, pyridinium ions in the (stoichiometric) salt occupy two crystallographically distinct sites in roughly equal numbers, it is difficult to explain why similar splittings are not observed in the corresponding peaks (at 1585 and 1490 cm^{-1}) for the N-deuterated compound. This phenomenon evidently requires further investigation. To confirm that the curvature in the calibration plot

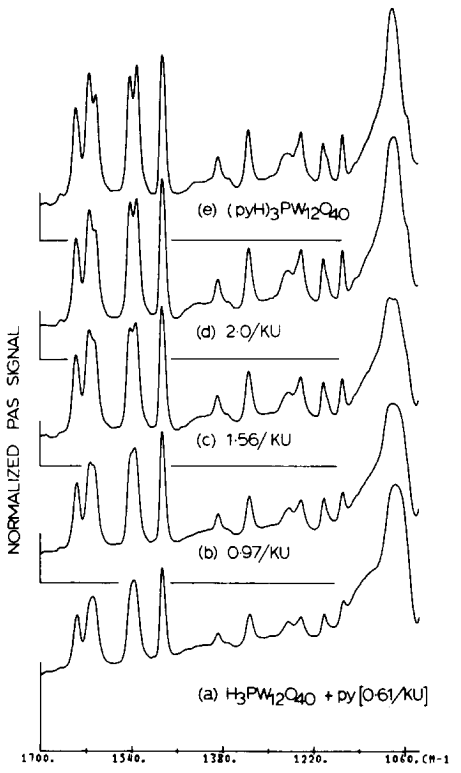

FIG. 4. Spectral details of $H_3PW_{12}O_{40}$ after sorption of pyridine: (a) 0.61 py/KU; (b) 0.97 py/KU; (c) 1.56 py/KU; (d) 2.0 py/KU; and (e) pyridinium salt for comparison.

was a genuine saturation effect and not associated with the splitting of the 1537-cm^{-1} band, the adjacent band at 1485 cm^{-1} was selected as a reference, showing no splitting. The peak area ratio A_{1537}/A_{1485} remained constant within experimental error (1.8 ± 0.1) across the whole range of pyridine loading, as would be expected for single bands of similar initial height (extinction coefficient) and ir (modulation) frequency (*12*).

2. *Pyridine on the Heteropoly Salts*

Previous studies (*1*), using NH_3 as probe, have revealed that the ammonium, aluminum, and sodium 12-phosphotungstates as prepared (*3a*) exist in (partial) Brønsted acid salt form, which may account for their intrinsic activity in methanol conversion. Characterization using pyridine should provide valuable complementary information concerning the type, amount, and relative strength of acidic sites in these salts. By analogy with the NH_4^+ salt examined earlier (*1*), the relative peak heights in the PAS spectra of the pyridinium salt (outgassed at various temperatures) and those obtained by dosing pyridine onto $H_3PW_{12}O_{40}$ indicated that this salt also might be substoichiometric. When peak area ratios were measured and reference made to the calibration curve, this was indeed found to be the case, with values of 2.6, 2.7, 2.2, and 2.0 pyH^+/KU, determined after evacuation at 25, 150, 250, and 350°C, respectively. The adjusted molecular formula for this salt from elemental (CHN) analysis (preevacuated at 150°C) was $(C_5H_5NH)_{2.7}H_{0.3}PW_{12}O_{40}$, in good agreement with that estimated by PAS under the same pretreatment conditions. The apparent trend of decreasing pyridinium ion content with increasing temperature of evacuation suggests the occurrence of pyridine desorption, a process which may possibly serve as an index, albeit qualitative, of the Brønsted acid strength of this salt. When a sample (2.0 pyH^+/KU) was exposed to excess pyridine directly at 250°C, the limiting volumetric uptake was significantly less than that required to form the stoichiometric salt and the peak area ratio, measured after evacuation at 150°C, confirmed that the pyridinium ion content was still less than stoichiometric (2.2 pyH^+/KU). However, when samples were given treatment similar to that undergone by $H_3PW_{12}O_{40}$ in the generation of the calibration curve, i.e., exposure to pyridine at room temperature followed by heating up to 150°C and evacuation, the stoichiometric pyridinium salt was obtained. As the evacuation conditions, after exposure, were identical in both methods, the discrepancy cannot be accounted for by thermal desorption. Hence, instead of the effect expected from higher temperature exposure, i.e., that of increasing the rate of pyridinium ion formation by accelerated

TABLE 1

Nominal molecular formula (BET surface area, $m^2 g^{-1}$)	Residual proton content (H^+/KU) using pyH^+ formation				Adjusted molecular formula	
	Treatment 1	Treatment 2			Calculated from pyH^+ formation (PAS; treatment 2, 150°C evacuation)	Calculated from elemental analysis [in parenthesis][a]
	Exposed at 250°C, cooled to 150°C, and evacuated	Exposed at 25°C, heated to stated temperature, and evacuated				
		150°C	250°C	350°C		
$AlPW_{12}O_{40}$ (5.5) (*3a*)	0.26 (1.35)[b]	1.24	1.10	1.06	$Al_{0.59}H_{1.24}PW_{12}O_{40}$	$Al_{0.58}H_{1.26}PW_{12}O_{40}$ [0.55% Al]
$(NH_4)_3PW_{12}O_{40}$ (~130) (*3b*)	0.22 (0.40)[b]	0.25	0.22	0.18	$(NH_4)_{2.75}H_{0.25}PW_{12}O_{40}$	$(NH_4)_{2.6}H_{0.4}PW_{12}O_{40}$ [2.6% N]
$Na_3PW_{12}O_{40}$ (6.2) (*3a*)	0.07 (0.32)[b]	0.35	0.25	0.06	$Na_{2.65}H_{0.35}PW_{12}O_{40}$	$Na_{2.88}H_{0.12}PW_{12}O_{40}$ [2.25% Na]

[a] Values quoted are the means of duplicates.
[b] Corresponding values (H^+/KU) determined using NH_3 under the same conditions.

diffusion of pyridine through the bulk, this treatment, on the contrary, appears to inhibit penetration by some other overriding mechanism, possibly structural or steric in origin. Turning to the other salts, the above behavior was found to be the general case and not specific to the pyridinium salt. After preevacuation at 350°C and exposure to pyridine directly at 250°C, followed by evacuation at 150°C, the estimates of Brønsted acidity via formation of the pyridinium ion (Table 1, column 1) were markedly lower than the corresponding values obtained using NH_3 (in parentheses). To emphasize the difference in absorptive behavior between pyridine and NH_3 under these conditions, the Al^{3+} salt (Fig. 5a) was first exposed to excess pyridine at 250°C for 1h, (Fig. 5b) followed by exposure to NH_3 under the same conditions (Fig. 5c). The residual proton content determined from NH_4^+ ion formation (~1.2 H^+/KU) was much greater than that obtained from pyH^+ formation (~0.2 H^+/KU) and only slightly less than that measured in the absence of presorbed pyridine. However, when the salts were exposed to pyridine at 25°C and then heated up to 150°C and evacuated, the estimates for the Al^{3+} and Na^+ salts were increased ~fivefold (Table 1, column 2), now showing good agreement with the values obtained using NH_3. Curiously, the re-

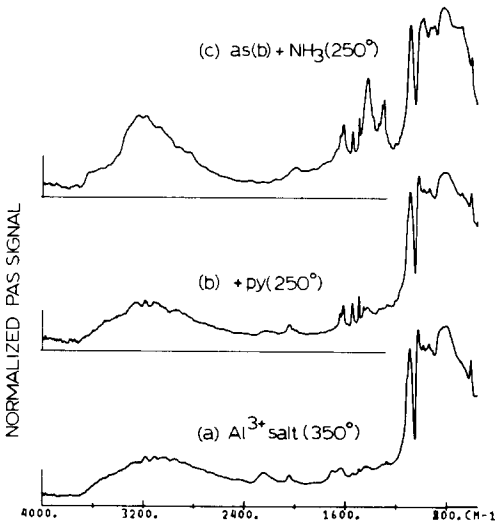

FIG. 5. (a) Al^{3+} salt (preevacuated at 350°C); (b) as (a) after exposure to excess pyridine at 250°C and evacuation at 150°C; (c) as (b) after exposure to excess NH_3 at 250°C and evacuation at 150°C.

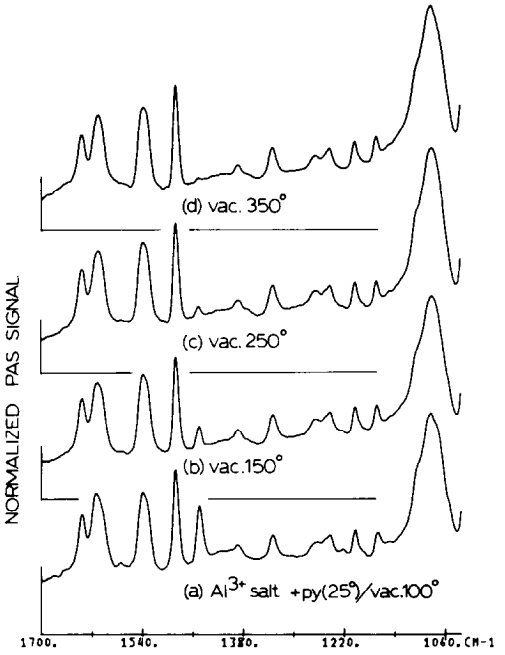

FIG. 6. Al^{3+} salt (preevacuated at 350°C) after exposure to excess pyridine at 25°C, followed by evacuation for 1 h at (a) 100°C, (b) 150°C, (c) 250°C, and (d) 350°C.

sidual proton content of the NH_4^+ salt thus determined showed virtually no improvement, remaining at about half of the NH_3 value. Volumetric uptakes were generally consistent with the PAS data (except in the case of the Al^{3+} salt), confirming that only the protonated species was formed with no evidence for other types of bound pyridine. Adopting the latter treatment as the most reliable for probing total proton content using pyridine, the adjusted molecular formula for the Al^{3+} salt (assuming charge balance by Al^{3+}) is in good agreement with that estimated by elemental analysis (assuming charge balance by protons). The proton content in the Na^+ salt, estimated using pyridine, is also believed to be accurate as it is in close agreement with that determined using NH_3 (*1*). The minor discrepancy between the molecular formulae determined by PAS and elemental analysis is thought to arise from an erroneous assumption that the salt is completely pure. Spectral evidence for the CO_3^{2-} ion has already been observed (*1*), and in view of the wide (×50) difference in the formula weights of CO_3^{2-} and $PW_{12}O_{40}^{3-}$, even slight contamination by the former ion would produce an artificially high Na^+ content and introduce an error in the formula calculated from elemental analysis. The most serious discrepancy occurs in the NH_4^+ salt and the use of pyridine to determine proton content in this case would appear ill-advised. Possible reasons for the anomalous behavior of the NH_4^+ salt will be discussed later.

In the Al^{3+} salt, a band characteristic of coordinately (Lewis)-bound pyridine (*6*) was evident at 1450 cm^{-1} after evacuation at 100°C (Fig. 6a), in addition to the familiar bands due to the pyridinium ion. Figures 6b–d illustrate the effect of evacuation for 1 h at 150, 250, and 350°C, respectively. The band at 1450 cm^{-1} is reduced already at 150°C but is still just detectable at 350°C. As evidence has already been found, using NH_3, for Lewis acidity in this salt, and ascribed to Al^{3+} ions in the bulk (*1*), the band at 1450 cm^{-1} may originate from the corresponding Al^{3+} : py species.

The effect of increasing the evacuation temperature up to 350°C, after exposure of the heteropoly salts to pyridine, is apparently to reduce systematically the residual proton content (estimated as pyH^+, see Table 1). However, as the salts were preevacuated at 350°C, this effect cannot be due to loss of H^+ (as pyH^+) but rather is evidence for thermal desorption of pyridine, an effect already observed in the case of the pyridinium salt. Hence, these figures may be considered to reflect the relative strength of Brønsted acid sites in the respective salts. The Al^{3+} salt evidently possesses the highest concentration of, and possibly the strongest, acidic sites of all the salts under examination, whereas the Na^+ salt has the least, and weakest, acidic sites. The protons in the NH_4^+ salt appear to be of similar strength to those in the Al^{3+} salt, albeit fewer in number.

DISCUSSION

1. Pyridine on $H_3PW_{12}O_{40}$

Previous work (*1*) has shown that the small NH_3 molecule readily penetrates the bulk structure of these heteropoly compounds and quantitatively converts any protons to NH_4^+, thus providing the basis for a valuable method to measure total Brønsted acidity. The results obtained in the present investigations, however, demonstrate that sorption of the larger pyridine molecule into the bulk structure is a more complex process, being apparently strongly dependent on the secondary structure of the heteropoly compounds, i.e., the structural arrangement of anions and cations, which itself may vary with the nature and number of sorbate molecules. This is well-illustrated in the case of 12-tungstophosphoric acid, $H_3PW_{12}O_{40}$, which readily sorbs up to 6 pyridine molecules/KU to form the dimer ion salt $(py_2H)_3PW_{12}O_{40}$. The continuum in the PAS spectrum of this salt extends across almost the entire mid-ir region, 3600–550 cm^{-1}, a feature characteristic of groupings with symmetrical polarizable hydrogen bonds subject to a large statistical distribution of field strength (via induced dipole interactions and/or proton dispersion forces), conditions prevalent in amorphous or liquid systems (*13*). In contrast, in crystals, containing, e.g., $H_5O_2^+$, the same crystal field is present at the H-bonds and these (bonds) have the same distances and orientations to one another. Thus, instead of a continuum, discrete, though broad, bands are observed (*14*). Consistent with the PAS data, there is independent evidence from XRD that the crystalline structure of $H_3PW_{12}O_{40}$ is lost on exposure to excess pyridine (*15*), an unsurprising result in view of the high solubilities reported for heteropoly acids in polar solvents (*16*).

The two broad absorption features at 2500 and 2000 cm^{-1} in the spectrum of $H_3PW_{12}O_{40}$ exposed to excess pyridine (Fig. 1b) cannot be readily assigned at this stage. Although corresponding peaks were observed by Clements and Wood (*8*), they reported no ir continuum and attributed this doublet to the $(N..H..N)^+$ group in the (py_2H^+) dimer ion. As the bands in the PAS spectrum appear to develop at the expense of bands at ~2240 and 1640 cm^{-1}, associated with lattice water (*1*), their origin in species such as $(PyH..OH_2)^+$ cannot be ruled out. However, similar features have also been observed in nonaqueous systems by other workers (*17*). Strong H-bonding interactions with the anion in pyridinium salts have been reported to cause shifts of the $\overset{+}{N}$–H stretching vibration to below 2500 cm^{-1} (*7*), and there is some evidence in Fig. 1b that the pyridinium ion is not entirely converted to the dimer as weak bands are still observed at ~3100 and ~1540 cm^{-1}. Hence, it is possible that, in addition to the $(py_2H)^+$ dimer ion, relatively small amounts of species such as $(py_1H...py_2)^+$ may be formed in which the (N–H...N) band is still relatively strong but asymmetrical and less polarizable. Such bonds are known to produce ir continua over a restricted range or broad bands in the region characteristic of those of the monomer perturbed by strong H-bonding (*9*). Further work is evidently required to elucidate this intriguing phenomenon.

2. The Value of Pyridine as a Probe of Acidity in Heteropoly Salts

The use of pyridine, as a complementary base to NH_3, for the quantitation of Brønsted acidity in heteropoly salts appears possible only in certain cases and is generally less convenient and reliable in view of the more stringent experimental conditions under which data must be obtained. Nonetheless, studies of the interaction of pyridine with the salts under investigation has yielded data which are generally consistent with those obtained previously using NH_3 (*1*). The nonstoichiometry associated with the Al^{3+} salt and, to a lesser extent, the Na^+ salt has been confirmed but the restricted penetration of the larger pyri-

dine molecule into the bulk of these salts at elevated temperature is not readily understood. A semiquantitative estimate of the depth of penetration, in terms of molecular layers of the catalyst, can be made on the basis of its surface area and the fraction of the total proton content probed by pyridine at 250°C. It has been calculated (*2*) that a molecular dispersion of $H_3PW_{12}O_{40}$ may attain a surface area of 650 $m^2\ g^{-1}$. Hence, the measured surface areas for the Al^{3+} and Na^+ salts (5 $m^2\ g^{-1}$, see Table 1) indicate that the crystallites contain roughly 100 molecular layers. Pyridine evidently detects ~20% of the available protons at 250°C (see Table 1), implying that penetration to a depth of ~20 layers is possible. Arguments based on steric hindrance by the effect of temperature on the aperture size of the diffusional pathways through the bulk appear untenable if the analogy is drawn with zeolites. The encapsulation of gases in molecular sieves by treatment at high temperature is a well-known phenomenon and has been attributed to the effective increase in aperture size resulting from the greater vibrational amplitude of oxygen atoms surrounding the apertures (*18*). A better explanation may be that the absorbed pyridine itself acts as an effective block to diffusion at the higher temperature due to its more rapid reaction with protons and resultant anchoring (as pyridinium ion) in the uppermost surface layers. The anomalous behavior of the NH_4^+ salt cannot be accounted for in the same way, as the degree of penetration is virtually independent of the conditions of absorption. Indeed, the high surface area of this salt (>100 $m^2\ g^{-1}$, see Table 1) indicates that penetration is much more severely restricted, in this case to ~2 layers, a result which provides good evidence in support of the earlier contention (*1*) that the dimensions of diffusional pathways in the NH_4^+ salt may be less in view of its smaller lattice parameter and larger cationic radius relative to the Al^{3+} and Na^+ salts. The behavior of this system stands in sharp contrast to that of $H_3PW_{12}O_{40}$ and emphasizes the likelihood that heteropoly compounds may exhibit a wide range of (bulk) diffusional characteristics depending on the catalytic reaction, i.e., the size distribution of reactant/product molecules, of interest.

Despite these peculiarities, pyridine complements, NH_3 by virtue of its weaker basicity. The results of thermal desorption of pyridine provide information on the relative Brønsted acid strength of these salts which is qualitatively consistent with data from indicator methods (*3a,b*). Thus, the low activity in methanol conversion but significant dehydration activity exhibited by the Na^+ salt may be a consequence of its weaker Brønsted acid sites. By the same token, the high activities of the NH_4^+ and Al^{3+} salts in methanol conversion may derive from their strong acid sites. Similar qualitative trends of acid strength with cracking/polymerization versus dehydration reactions in general are well-documented (*19*). In view of their similar acid strengths and widely different capacities to sorb pyridine, the origin of selectivity differences in the NH_4^+ and Al^{3+} salts may lie in surface vs bulk factors, or the presence of Lewis acidity in the latter salt, as discussed earlier (*1*). Final judgment, however, must await the results of selective poisoning experiments.

In summary, it is evident that the sorption of pyridine into heteropoly compounds is a relatively complex process in which the nature of the cation exerts an important influence. The cation size, and charge (as reflected in the cation/anion stoichiometric ratio) almost certainly play important roles in establishing steric barriers to facile migration of pyridine, but may also exert indirect control through perturbation of the symmetry properties of the secondary structure (as in the case of the pyridinium salt), and through the capacity of the crystal lattice to accommodate sorbates by expansion of the interstitial space, as governed by lattice energy considerations (reflected in solubility data). The presence

of protons may have the dual effect of encouraging diffusion via the establishment of short-range attractive forces (on the lone pair of electrons of the nitrogen atom in the pyridine molecule) while inhibiting diffusion through the steric barrier exerted by the "anchored" pyridinium ions so formed. Whether the smaller methanol molecule, and related intermediates and reaction products, are also subject to such a degree of diffusional control is yet to be explored.

ACKNOWLEDGMENTS

The authors thank Dr. B. K. Hodnett and Dr. J. M. McMonagle for their kind assistance in providing X-ray diffractograms and for useful discussion during the experimental work. The authors gratefully acknowledge the Natural Sciences and Engineering Research Council for financial support.

REFERENCES

1. Highfield, J. G., and Moffat, J. B., *J. Catal.* **88,** 177 (1984).
2. Hayashi, H., and Moffat, J. B., *J. Catal.* **77,** 473 (1982).
3. (a) Hayashi, H., and Moffat, J. B., *J. Catal.* **81,** 61 (1983); (b) **83,** 192 (1983).
4. Knozinger, H., "Advances in Catalysis," Vol. 25, p. 184. Academic Press, New York, 1976.
5. Misono, M., Mizuno, N., Katamura, K., Kasai, A., Konishi, Y., Sakata, K., Okuhara, T., and Yoneda, Y., *Bull. Chem. Soc. Jpn.* **55,** 400 (1982).
6. Parry, E. P., *J. Catal.* **2,** 371 (1963).
7. Cook, D., *Canad. J. Chem.* **39,** 2009 (1961).
8. Clements, R., and Wood, J. L., *J. Mol. Struct.* **17,** 265 (1973).
9. Zundel, G., *in* "The Hydrogen Bond" (P. Schuster, G. Zundel, and C. Sandorfy, Eds.), Vol. 2, Chap. 15 and references cited therein. North-Holland, Amsterdam, 1976.
10. Highfield, J. G., and Moffat, J. B., in preparation.
11. Azaroff, L. V., "Elements of X-Ray Crystallography," p. 490. McGraw–Hill, New York, 1968.
12. Chalmers, J. M., Stay, B. J., Kirkbright, G. F., Spillane, D. E. M., and Beadle, B. C., *Analyst (London)* **106,** 1179 (1981).
13. Zundel, G., *in* "The Hydrogen Bond" (P. Schuster, G. Zundel, and C. Sandorfy, Eds.), Vol. 2, p. 747. North-Holland, Amsterdam, 1976.
14. Gilbert, A. S., and Sheppard, N., *J. Chem. Soc. Faraday 2* **69,** 1628 (1973).
15. Hodnett, B. K., and Moffat, J. B., unpublished results.
16. Tsigdinos, G. A., *Top. Curr. Chem.* **76,** 1 (1978).
17. Pawlak, Z., and Sobczyk, L., "Advances in Relaxation Processes," Vol. 6. Elsevier, Amsterdam/New York, 1973.
18. Breck, D. W., "Zeolite Molecular Sieves," pp. 633ff. Wiley–Interscience, New York, 1974.
19. Tanabe, K., "Solid Acids and Bases," pp. 119ff. Academic Press, New York, 1970.